

FENDI: High-Fidelity Entanglement Distribution in the Quantum Internet

Huayue Gu[‡], *Student Member, IEEE*, Zhouyu Li[‡], *Student Member, IEEE*, Ruozhou Yu, *Senior Member, IEEE*,
Xiaojian Wang, *Student Member, IEEE*, Fangtong Zhou, *Student Member, IEEE*,
and Jianqing Liu, *Member, IEEE*

Abstract—A quantum network distributes quantum entanglements between remote nodes, which is key to many quantum applications. However, unavoidable noise in quantum operations could lead to both low throughput and low quality of entanglement distribution. This paper aims to address the simultaneous exponential degradation in throughput and quality in a buffered multi-hop quantum network. Based on an end-to-end fidelity model with worst-case (isotropic) noise, we formulate the high-fidelity remote entanglement distribution problem for a single source-destination pair, and prove its NP-hardness. To address the problem, we develop a *fully polynomial-time approximation scheme* for the control plane of the quantum network, and a distributed data plane protocol that achieves the desired long-term throughput and worst-case fidelity based on control plane outputs. To evaluate our algorithm and protocol, we develop a discrete-time quantum network simulator. Simulation results show the superior performance of our approach compared to existing fidelity-agnostic and fidelity-aware solutions.

Keywords—Quantum network, entanglement routing, entanglement fidelity, network optimization, approximation algorithm

I. INTRODUCTION

A quantum network enables efficient communication of quantum information based on the principle of quantum entanglement [25]. The ability to transmit quantum information between remote nodes is key to many astonishing quantum applications, such as quantum key distribution (QKD) [4], distributed quantum computing [6], [12], quantum cryptography [34] and quantum internet-of-things [11].

While the concept has been proposed for years, practical quantum networking has come around the corner with several recent real-world implementations [13], [21], [32], [35], [45]. Though current systems are built in ideal conditions and small-scale in nature, research has looked into how such small-scaled networks could be possibly extended to a fully-fledged, global-scale quantum internet [48]. A key functionality of a quantum internet is to distribute entangled qubits between remote nodes across long distances. For instance, an entangled pair of photons can teleport one quantum bit between a pair of nodes that are arbitrarily far away from each other. Future applications would require a steady stream of high-quality entanglements between arbitrary remote ends.

A quantum network distributes entanglements by *entanglement generation* and *entanglement swapping*. If a quantum link connects a pair of nodes, a remote entanglement between

them can be generated by preparing a pair of entangled photons, and directly sending each photon to one node. The generated entanglements can be further concatenated at joint intermediate nodes via entanglement swapping to establish entanglements between indirectly connected nodes. In this way, each end-to-end entanglement is thus generated along an *entanglement path* in a quantum network.

As entanglements are a critical resource, attention has been drawn to designing efficient entanglement distribution protocols. A quantum network has unique characteristics imposed by the underlying physics or technology deficits. Specifically, unavoidable noise in quantum systems can lead to failures or degraded quality in quantum operations and can affect *communication efficiency* in a quantum network. To mitigate this, existing work has studied *efficient entanglement routing* to find entanglement paths with maximum success probability. Along each path, resources such as optical channels are prepared to establish end-to-end entanglements, similar to classical bufferless virtual circuit switching.

In this paper, we study entanglement distribution in a *buffered quantum network*. Buffers are important in the classical Internet for smoothing traffic and matching speeds between different components in a network. Owing to recent advances in quantum memories [29], quantum networks with large-capacity, long-lived buffers could be within reach in the near future, which have significant advantages considering traffic throughput and reliability. For instance, an optimal entanglement distribution rate can be achieved by a packet-switching, hop-by-hop protocol in a buffered quantum network [14] that is not viable in a bufferless one.

The issue with packet switching in a buffered network is the difficulty in providing high quality-of-service (QoS). In a quantum network, an important QoS metric is the quality (*aka* fidelity) of the distributed entanglements. Low fidelity results in low communication efficiency due to excessive error correction needed, even when the entanglement distribution rate is high. This paper studies how to achieve high fidelity while maintaining a high entanglement distribution rate. Our proposed solution, named **FENDI**, includes a *control plane algorithm* for computing approximate solutions for high-fidelity entanglement distribution, and a *data plane protocol* for implementing the solutions in a buffered quantum network. Our main contributions are as follows:

- To our best knowledge, we are the first to formulate high-fidelity remote entanglement distribution (HF-RED) in a *general-topology buffered quantum network*.
- We prove HF-RED to be NP-hard, and propose a *fully polynomial-time approximation scheme (FPTAS)*. This is the first algorithm with theoretical guarantee for both the entanglement distribution rate (EDR) and worst-case fidelity in a general-topology quantum network.

[‡] Both authors contributed equally to this research.

Gu, Li, Yu, Wang, Zhou and Liu ({hgu5, zli5, ryu5, xwang244, fzhou, jliu96}@ncsu.edu) are all with North Carolina State University, Raleigh, NC 27606, USA.

This research was supported in part by NSF grant 2304118. The information reported here does not reflect the position or the policy of the funding agency.

- We further design a data plane protocol that implements the solution of the control plane algorithm, and achieves the desired EDR and worst-case fidelity.
- We evaluate FENDI with a quantum network simulator, and show its advantages compared to state-of-the-arts.

Organization: §II reviews background and related work. §III introduces quantum network basics. §IV formulates HF-RED in a buffered quantum network, and proves its NP-hardness. §V and §VI present our control and data plane designs respectively with theoretical analysis. §IV-D presents simulation results. §VIII concludes the paper.

II. BACKGROUND AND RELATED WORK

As with any emerging technology, early work in quantum networking focused on feasibility demonstration in ideal situations. Multi-hop entanglement distribution was first demonstrated on repeater chains both in theory and in reality [8], [21], [22], [38]. Much of the literature has since then focused on deriving analytical and simulation models for quantum repeater chains [7], [17], [37]. Other specialized topologies include lattices [31], star [41] and ring-like topologies [9], [36]. In reality, a quantum internet is unlikely to have such ideal topologies due to physical and geographical limitations.

Recent studies have focused on *entanglement routing* in general-topology quantum networks [10], [15], [28]. A traditional approach was to find paths with the highest success probabilities using modified shortest path algorithms [40]. Shi *et al.* [37] first showed that maximum-success paths do not lead to the highest throughput. They developed two algorithms Q-CAST and Q-PASS based on an optimal single-path routing metric. Zhao *et al.* [48] proposed an algorithm to achieve higher throughput by provisioning redundant intermediate entanglements for swapping in each time slot. Zeng *et al.* [47] proposed an integer programming-based solution using branch-and-price with very limited quantum memories. Above works only considered the success probability in routing but ignored the quality (fidelity) of entanglements. Zhao *et al.* [49] first studied fidelity-aware entanglement routing. They derived an end-to-end fidelity model based on *bit flip errors*, and proposed a purification-based fidelity-aware routing algorithm based on heuristic path selection, linear programming and rounding. We note that no existing work has theoretical guarantee considering both EDR and fidelity for multi-path routing in a general-topology quantum network.

A common choice in the above studies is that all generation and swapping must be completed in one time slot. If the time expires or any operation fails, all intermediate entanglements must be dropped. This corresponds to the *bufferless* assumption in quantum networks, due to the very short coherence time of available quantum memories. However, a recent study has demonstrated quantum memories with up to 1 hour coherent time [29]. This opens up doors for a buffered quantum network where a large number of long-lived quantum memories can act as intermediate buffers to store intermediate entanglements and realize the full capacity of a quantum network. Askarani *et al.* [2] presented a multi-platform quantum network with the analysis of entanglement distribution rate and expected fidelity by constructing the quantum repeater chains in the protocol. Dai *et al.* [14] proposed the first *optimal remote entanglement distribution* protocol realizing optimal throughput (without purification) in a buffered quantum network. Their protocol stores intermediate

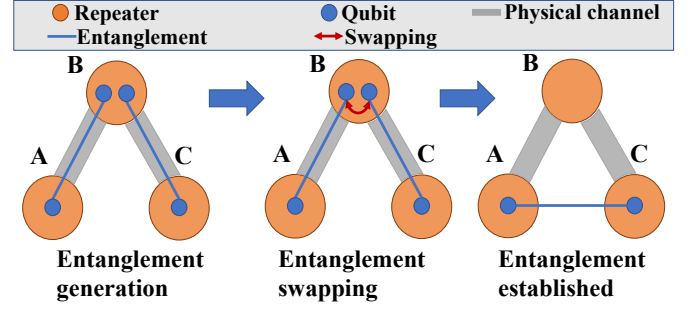


Fig. 1: Basic quantum network operations: entanglement generation and entanglement swapping.

entanglements in buffers until swapping, thus smoothing the entanglement traffic. Dai *et al.* further analyzed the quantum queueing delay for a single quantum channel in [16]. It is notable that (*bufferless*) *entanglement routing* is a special case of (*buffered*) *entanglement distribution*. Therefore, the ORED protocol also provides an upper bound on the maximum throughput achievable by any entanglement routing protocol (without purification). Unfortunately, the ORED protocol has no guarantee in terms of fidelity of the distributed entanglements, and hence their protocol may not be practical due to low fidelity of distributed entanglements. This motivates our study of fidelity-aware entanglement distribution.

III. QUANTUM NETWORK BASICS

A. Basic Quantum Informatics

Consider a common 2-state quantum system with orthonormal basis states $|0\rangle$ and $|1\rangle$. A quantum bit (*qubit*) is a superposition of $|0\rangle$ and $|1\rangle$, written as $|b\rangle = \alpha|0\rangle + \beta|1\rangle$, satisfying $\alpha^2 + \beta^2 = 1$. A perfect measurement on $|b\rangle$ yields classical state 0 with probability α^2 and 1 with probability β^2 . A two-qubit system is described by a superposition of four basis states $|00\rangle$, $|01\rangle$, $|10\rangle$ and $|11\rangle$. Let $|b_1b_2\rangle = \alpha_{00}|00\rangle + \alpha_{01}|01\rangle + \alpha_{10}|10\rangle + \alpha_{11}|11\rangle$, such that $\alpha_{00}^2 + \alpha_{01}^2 + \alpha_{10}^2 + \alpha_{11}^2 = 1$. Simultaneous measurement on the two qubits will yield 00 with probability α_{00}^2 , 01 with probability α_{01}^2 , 10 with probability α_{10}^2 , and 11 with probability α_{11}^2 , respectively.

A maximally entangled pair (called a Bell pair) is a two-qubit system in one of the four *Bell states*: $|\Phi^\pm\rangle = \frac{1}{\sqrt{2}}(|00\rangle \pm |11\rangle)$, and $|\Psi^\pm\rangle = \frac{1}{\sqrt{2}}(|01\rangle \pm |10\rangle)$. A Bell pair is *maximally entangled* since it only contains two of the four basic states with equal probability, where in both states the two qubits are perfectly correlated. For instance, in state $|\Psi^+\rangle$, if one of the qubits measures into x , then the other qubit must measure into $(1-x)$, for $x \in \{0, 1\}$. Bell pairs form the basis of two-party quantum communications: if Alice and Bob each holds one of the qubits, they can use this pair to send quantum information via *local operations and classical communication* (LOCC).

B. Quantum Internet

A quantum internet is a distributed facility distributing remote entangled qubit pairs (*ebits*) between source-destination pairs, via entanglement generation and swapping. In Fig. 1, two *elementary ebits* are generated along links A–B and B–C respectively. To swap, B entangles and measures its two local qubits and sends the measurement result to C via classical communications. According to the result, C applies a unitary operation on its qubit. Two qubits at A and C are then

entangled in the desired state without interacting with each other. This can be done recursively along a path until an end-to-end ebit between source and destination is established¹.

Formally, we model a quantum internet with an undirected graph $G = (N, L)$, where N is the set of quantum repeaters, and L is the set of physical channels (links) between repeaters. Each link $l \in L$ has a capacity $c_l \in \mathbb{Z}^+$, denoting the number of ebits that can be generated along the link in unit time; \mathbb{Z}^+ denotes the positive integer set. For simplicity, we call ebits generated along a physical channel *elementary ebits*.

C. Noise and Fidelity

Unsuccessful operations: In a quantum network, both entanglement generation and swapping can fail, which can lead to degraded end-to-end throughput of ebits. To model this, each link $l \in L$ is associated with a probability $p_l \in (0, 1]$ of successfully generating an elementary ebit. Each repeater $n \in N$ is further associated with a probability $q_n \in (0, 1]$ for successfully performing swapping. A swapping failure consumes the two source ebits without generating a target ebit. For instance, current BSM based on linear optical techniques can only distinguish three over the four Bell states [27], leading to (detectable) failure in swapping itself with a measurable failure probability.

Inaccurate operations or noisy channel: For a successfully generated ebit in a mixed state M , let $|\Phi^+\rangle$ be its intended pure state². The mixed state can be resulted from an arbitrary noisy channel or noise in the quantum operations; we assume a worst-case isotropic error model [42], as compared to the bit flip error model in [49]. The accuracy of M is measured by its *fidelity* as $F \triangleq \langle \Phi^+ | M | \Phi^+ \rangle$, denoting the probability that state M is in the desired state $|\Phi^+\rangle$. As shown by Bennett *et al.* [5], an arbitrary mixed state M with fidelity F can be transformed to a Werner state with the same fidelity via *random bilateral rotations* (RBR). The Werner state with F is defined as

$$W_F = F|\Phi^+\rangle\langle\Phi^+| + \frac{1-F}{3}(|\Phi^-\rangle\langle\Phi^-| + |\Psi^+\rangle\langle\Psi^+| + |\Psi^-\rangle\langle\Psi^-|). \quad (1)$$

This Werner state can be viewed as a mixture of the pure state $|\Phi^+\rangle$ with isotropic noise [42]. Hereafter, we assume all elementary and intermediate mixed ebits are transformed to the Werner state in Eq. (1) before further swapping.

For an elementary ebit established along a physical channel, its fidelity is decided by the quantum circuit that generates the entanglement, and the channel noise during distribution. Hence for each physical link $l \in L$, we define F_l as the fidelity of elementary ebits generated along l . Given two ebits with fidelity F_1 and F_2 respectively, consider a *perfect* entanglement swapping is performed between the two ebits, meaning no error (fidelity loss) could happen during swapping. The swapping could be implemented as a Bell state measurement, which includes a CNOT gate followed by two single-qubit gates. Note that even if the swap (BSM) is perfect, it may still fail due to the two source ebits not being in the desired state, thus leading to measurement error. Two cases may happen in a successful swap: 1) both ebits are in the desired state with probability (fidelity) $F^* = F_1 F_2$, in which case the

swapped ebit is also in the desired state; 2) both ebits are not in the desired state but have equal states, with probability $F^{**} = 3 \frac{(1-F_1)}{3} \frac{(1-F_2)}{3}$, in which case the swapped ebit is not in $|\Phi^+\rangle$ but in one of the other Bell states, which can be transformed to $|\Phi^+\rangle$ via LOCC [5]. In the other cases, the swapping fails because of unknown and unequal states of the two ebits.

By combining these cases, a *perfect* entanglement swapping will result in a new ebit with fidelity F' [20], where

$$F' = \frac{1}{4} \cdot \left(1 + \frac{(4F_1 - 1)(4F_2 - 1)}{3} \right). \quad (2)$$

To facilitate expression, we define $W_l \triangleq \frac{4F_l - 1}{3}$ as the actual fidelity parameter of each link.

In practice, the swapping operation is also noisy or *imperfect*, and hence additional fidelity loss will be incurred during swapping. Such fidelity loss is correlated with the reliability of BSM, 1-qubit operation, and 2-qubit operation. For instance, if an entanglement swapping is performed with two elementary ebits with F_1 and F_2 at a node n where the accuracy of BSM and probabilities of ideal 1-qubit, 2-qubit operations are α_n , $o_{1,n}$, and $o_{2,n}$, respectively, the fidelity of a successfully generated ebit after swapping [20] is

$$F' = \frac{1}{4} \cdot \left(1 + 3o_{1,n}o_{2,n} \frac{4\alpha_n^2 - 1}{3} \frac{4F_1 - 1}{3} \frac{4F_2 - 1}{3} \right). \quad (3)$$

To facilitate expression, we define $W_l \triangleq \frac{4F_l - 1}{3}$ and $W_n \triangleq o_{1,n}o_{2,n} \frac{4\alpha_n^2 - 1}{3}$, the fidelity of a successfully generated ebit after swapping is

$$F' = \frac{1}{4} \cdot (1 + 3W_1 W_2 W_n). \quad (4)$$

Assume an end-to-end ebit is established by swapping elementary ebits created along links $\{l_1, l_2, \dots, l_{X+1}\} \subseteq L$ recursively at nodes $\{n_1, n_2, \dots, n_X\} \subseteq N$. Recursively applying Eq. (4), the end-to-end fidelity of the ebit is

$$F^{\text{EE}} = \frac{1}{4} \cdot \left(1 + 3 \prod_{i=1}^{X+1} W_{l_i} \prod_{j=1}^X W_{n_j} \right). \quad (5)$$

Eq. (5) will serve as the basic tool to quantify and optimize the end-to-end fidelity of ebits distributed in a quantum internet.

IV. REMOTE ENTANGLEMENT DISTRIBUTION IN A BUFFERED QUANTUM NETWORK

A. Remote Entanglement Distribution (RED)

We are interested in designing a *remote entanglement distribution (RED)* protocol that can deliver high-fidelity ebits between a source-destination pair. All notations used in our design are summarized in Table I. In a RED protocol, quantum repeaters continuously generate ebits along physical channels, meanwhile each repeater simultaneously performs swapping between generated ebit pairs, resulting in a continuous stream of end-to-end ebits. RED differs from *entanglement routing* in that ebits may be stored in quantum memories at repeaters shortly, until another ebit that can form a pair is available for swapping. This alleviates the strict constraint in entanglement routing that every ebit must be either consumed in the same time slot, or discarded immediately due to decoherence.

Fig. 2 shows an example quantum network with buffers. A , B and C are three quantum repeaters, and there exist one ebit between $A-B$ and two ebits between $B-C$. In a buffered network, the two entangled qubits of each ebit are respectively

¹ Although entanglements are undirected, we use traditional network terms “source” and “destination” to denote an undirected pair of end nodes involved in quantum communications for simplicity.

² Since all Bell states are symmetric, we use $|\Phi^+\rangle$ as the target state without loss of generality throughout this paper.

TABLE I: Notation Table

Parameters	Description
$G = (N, L)$	undirected graph G with the set of nodes N and the set of links L
F_L	fidelity of elementary ebits along link l
c_l	capacity of link l
p_l	entanglement generation success probability
q_n	entanglement swapping success probability
$m:n$	entangled qubit pair of node m and node n
$m:n/z$	enode $m:n$ at a path segment length of z
Δ_{st}	expected EDR between s and t
Υ_{st}	end-to-end fidelity bound between s and t
$\zeta(p)$	ebits are distributed for each (s, t) -path p
$\zeta^\theta(p)$	maximum quantized path length of path p
ε	factor of the optimal length
θ	quantization factor
Z	quantized length bound
\mathbf{Z}	non-quantized length bound
ω	fidelity accuracy parameter
$\mathcal{E}_{m:n/z}$	input buffer to store ebits generated between $m:n$ by quantized length z
$\mathcal{D}_{k:n/z'}^{m:n/z}$	output buffer to store ebits between $m:n$ that will be contributed to generating ebits between other pairs between $k:n$
Variables	Description
η_{st}	the entanglement distribution rate of (s, t)
η_{st}^Z	the entanglement distribution rate between s and t with a path length bound Z
$f_{m:n}^{m:k}$	amounts of entangled qubit pairs of $m:k$ would be distributed to $m:n$ after entanglement swapping.
$f_{m:n/z}^{m:k/z'}$	number of ebits between $m:k$, with a path segment length of z' , which will contribute to swapping at node k to generate ebits between $m:n$ with a path segment length of z
$g_{m:n}$	amounts of ebits would be generated along physical link $m:n$ divided by the capacity c_{mn} of edge $m:n$

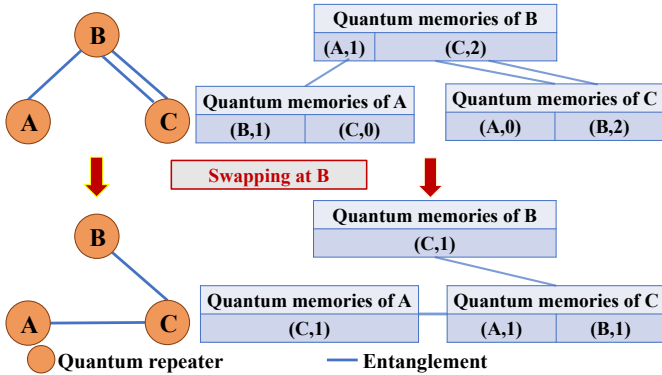


Fig. 2: Entanglement swapping with quantum memories as buffers. Each tuple (repeater, counter) in brackets represents a buffer at a node.

stored in buffers at its end-points after generation. For instance, the pair of entangled qubits between $A-B$ are stored in A 's buffer as $(B, 1)$, and B 's buffer as $(A, 1)$, respectively. To perform swapping, intermediate node B will retrieve the two local qubits belonging to ebits $A-B$ and $B-C$ from its own buffers, and swap the two local qubits. If it succeeds, the result will be conveyed to A and C . A will then move its local qubit from $(B, 1)$ to $(C, 1)$, and C will then move its local qubit from $(B, 2)$ to $(A, 1)$, which completes the swapping.

We make two assumptions of a future quantum internet:

Asm. 1. Each quantum repeater is equipped with sufficient quantum memories as buffers to store intermediately generated

ebits until next-step swapping is ready. \square

Asm. 2. Fidelity of ebits will not degrade over time. \square

Justification: We note that the current quantum hardware has not realized long-term quantum memories in large scale, though advances have preliminarily demonstrated long-term quantum memories in restricted lab settings, realizing high-fidelity entanglement storage for up to one hour without decoherence [29]. If both qubits in an entangled qubit pair are stored in quantum memories with over one hour coherence times, fidelity of the ebit will degrade almost negligibly in the normal time frame of ebit distribution (in milliseconds to seconds [37], [48], [49]) in a quantum internet. Combining experiences from the success of the traditional Internet [23], [24], the recent proposals on packet-switching quantum networks [18], [46], and projected future advances in quantum memory technology [19], [29], we argue that quantum buffers are both essential and promisingly realizable for building high-performance quantum internet in the future. This also aligns with the current research trend [33]. \square

B. Optimal RED without Fidelity Consideration

Given Assumptions 1 and 2, a RED protocol instructs quantum repeaters to generate and swap entanglements at pre-determined rates, and store ebits that are awaiting other ebits for swapping. Dai *et al.* [14] proposed an optimal RED protocol (ORED) to achieve the maximum EDR, which will serve as a component in our design. EDR is defined as the average number of established ebits between a source-destination pair in unit time for a given protocol. For completeness, we outline the optimal protocol. Following the notation in [14], we use $m:n$ interchangeably with (m, n) to denote an arbitrary pair of nodes $m, n \in N$, regardless of whether there is a physical link between them. Although an entanglement is non-directional, a pair $m:n$ implicitly represents a direction of any ebit between m and n that is used to construct an ebit between a source-destination pair $s:t$, in the same direction from s to t .

Define variables $f_{m:n}^{m:k} \geq 0$ and $f_{m:n}^{k:n} \geq 0$ for nodes $m, n, k \in N$, and $g_{m:n} \in [0, 1]$ for links $(m, n) \in L$. $f_{m:n}^{m:k}$ denotes the number of ebits established between nodes m and k that will be used for swapping to generate ebits between m and n , and similarly is $f_{m:n}^{k:n}$ defined. $g_{m:n}$ denotes the number of elementary ebits to be generated along the physical link (m, n) , divided by the capacity c_{mn} of the link. The following linear program (LP) computes the maximum EDR between a pair of nodes $s, t \in N$:

$$\max_{f, g} \quad \eta_{st} \triangleq I(s, t) - \Omega(s, t) \quad (6)$$

$$\text{s.t.} \quad f_{m:n}^{m:k} = f_{m:n}^{k:n}, \quad \forall k, m, n \in N; \quad (6a)$$

$$I(m, n) = \Omega(m, n), \quad \forall m, n \in N, \{m, n\} \neq \{s, t\}; \quad (6b)$$

where for $\forall m, n \in N$,

$$I(m, n) \triangleq 1_L(m, n) p_{mn} c_{mn} g_{m:n} + \sum_{k \in N \setminus \{m, n\}} \frac{q_k}{2} (f_{m:n}^{m:k} + f_{m:n}^{k:n}), \quad (6c)$$

$$\Omega(m, n) \triangleq \sum_{k \in N \setminus \{m, n\}} (f_{m:n}^{m:k} + f_{m:n}^{k:n}), \quad (6d)$$

and $1_L(m, n)$ is an indicator function of whether $(m, n) \in L$. Here $I(m, n)$ denotes the ebits generated between node pair $m:n$ (including elementary ebits and ebits generated by swapping), and $\Omega(m, n)$ denotes the ebits contributed by $m:n$ to

generating ebits between other node pairs via swapping. Note that the elementary ebits (first term in Eq. (6c)) are discounted by the generation probability p_{mn} of a link, and the ebits received from swapping at node k are discounted by node k 's swapping success probability q_k . Constraint (6a) enforces that the two node pairs $m:k$ and $k:n$, whose ebits will be swapped to form ebits for $m:n$, contribute equal amounts of ebits to the swapping. Constraint (6b) enforces an intermediate pair $m:n$ does not keep generated ebits, but contributes all ebits to further swapping to construct end-to-end ebits for (s, t) . A solution satisfying all constraints in Program (6) is called an *eflow*, and each pair $m:n$ is called an *enode*.

Theorem 1 ([14]). *Program (6) gives the maximum expected EDR that can be obtained by any RED protocol.* \square

Consider the graph $\mathcal{G} = (V, E)$ induced by an eflow, i.e., each vertex $v = m:n \in V$ is an enode with $I(m, n) > 0$, and each edge $e \in E$ denotes either $e = (m:k, m:n)$ with $f_{m:n}^{m:k} > 0$ or $e = (k:n, m:n)$ with $f_{m:n}^{k:n} > 0$. A proposition in [14] shows that if Program (6) is feasible, then there is always an optimal eflow such that the induced graph \mathcal{G} is a *directed acyclic graph* (DAG). Such an optimal eflow can be easily computed by adding a secondary objective of minimizing the sum of all variables in the program, on top of the primary objective of maximizing the EDR η_{st} . Hence from now on, we only assume working with eflows that induce DAG structures. Based on the solution to Program (6), Dai *et al.* [14] proposed an optimal opportunistic RED protocol that achieves the maximum EDR.

C. Characterizing End-to-End Fidelity of an Eflow

Despite delivering optimal EDR, the ORED protocol in [14] does not consider fidelity in ebit distribution. Fidelity is a key quantum metric in a quantum network with no classical equivalent, which quantifies how close the quantum state is to the desired state in the range between 0 and 1. For entanglement distribution over long distances and multiple hops, the end-to-end fidelity would decrease exponentially with the increased noise and distances [26]. In quantum applications, if fidelity of a quantum state is below a threshold, the state will no longer be usable. Low fidelity can further lead to incorrect qubit measurement, destroying the valuable quantum information and leading to communication errors and wastage of resources in the quantum network [39]. On the other hand, different from classical data which commonly requires error-free transmission, entanglements with non-perfect though sufficiently high fidelity can still be used for many quantum applications with quantum error correction. This is our main motivation for considering EDR and fidelity at the same time in entanglement distribution.

We propose a method for quantifying the end-to-end fidelity of ebits generated by an arbitrary eflow. Specifically, we first define a *primitive eflow*, similar to a path in a traditional network flow. We then propose an *eflow decomposition theorem* based on it.

Definition 1 (Pflow). *A primitive eflow (pflow) is a feasible eflow as defined in Program (6), which satisfies that: for every enode $m:n$, either $g_{m:n} > 0$, or there exists exactly one $k \in N$ such that $f_{m:n}^{m:k} = f_{m:n}^{k:n} > 0$, but not both.* \square

A pflow is *primitive* in that ebits at each enode $m:n$ is generated in exactly one way: either they are elementary ebits generated directly along link $(m, n) \in L$, or they are generated

Algorithm 1: Computing ebit generation ratios of a pflow

Input: Induced graph \mathcal{G} of an (s, t) -pflow

Output: Ebit generation ratios $\{\bar{g}_{m:n}, \bar{f}_{m:n}^{m:k}, \bar{f}_{m:n}^{k:n}\}$

```

1 Initialize all ratios to 0, and  $Q \leftarrow \{(s:t, 1)\}$ ;
2 while  $Q \neq \emptyset$  do
3    $(m:n, \psi) \leftarrow Q.pop()$ ;
4   if  $\nexists k$  such that  $(m:k, m:n) \in E$  then
5      $\bar{g}_{m:n} \leftarrow g_{m:n} + \psi/p_{mn}$ ;
6   else
7      $\bar{f}_{m:n}^{m:k} \leftarrow \bar{f}_{m:n}^{m:k} + \psi/q_k$ ,  $\bar{f}_{m:n}^{k:n} \leftarrow \bar{f}_{m:n}^{k:n} + \psi/q_k$ ;
8      $Q.push((m:k, \psi/q_k))$ ,  $Q.push((k:n, \psi/q_k))$ ;
9 return  $\{\bar{g}_{m:n}, \bar{f}_{m:n}^{m:k}, \bar{f}_{m:n}^{k:n}\}$ .
```

by swapping $m:k$ - and $k:n$ -ebits at a single intermediary k . A pflow naturally represents exactly one *path* in the quantum internet, along which the final (s, t) -ebits are generated. Let p be the path of a pflow. The end-to-end fidelity of ebits generated along p can be directly computed via Eq. (5).

Another property of a pflow is that the ratio between each variable $g_{m:n}$, $f_{m:n}^{m:k}$ or $f_{m:n}^{k:n}$, and the final objective value η_{st} , is fixed. Let $\bar{g}_{m:n}$, $\bar{f}_{m:n}^{m:k}$ and $\bar{f}_{m:n}^{k:n}$ be the ratios between the corresponding variables and the final objective value, i.e., EDR of the pflow. Given the induced graph \mathcal{G} of the pflow, these ratios can be computed as in Algorithm 1, by backtracking from enode $s:t$, which has a ratio of 1 (one generated $s:t$ ebit translates into one end-to-end (s, t) -ebit). For each enode $m:n$, its output ebit rate ψ is added to its input ebit rate(s), i.e., either $\bar{g}_{m:n}$ or $\bar{f}_{m:n}^{m:k}$ and $\bar{f}_{m:n}^{k:n}$, augmented by the corresponding expected ratios of $1/p_{mn}$ or $1/q_k$ respectively. Based on Algorithm 1, a pflow can essentially be defined by its induced graph \mathcal{G} , and a single objective value $\eta_{\mathcal{G}}$ assigned to this pflow.

Theorem 2 (Eflow decomposition). *An eflow with $\eta_{st} > 0$ can be decomposed into a polynomial number of pflows.* \square

Proof: We decompose an eflow as follows. Let \mathcal{G} be the induced graph of the eflow. We first find an induced graph $\mathcal{G}' \subseteq \mathcal{G}$ in which each enode $m:n \in \mathcal{G}'$ has either $g_{m:n} > 0$, or there is exactly one $k \in N$ such that $f_{m:n}^{m:k} = f_{m:n}^{k:n} > 0$, and $(m:k, m:n)$ and $(k:n, m:n)$ are both in \mathcal{G}' . Such a subgraph must exist due to the constraint of $I(m, n) - \Omega(m, n) = 0$ for every $m:n \neq s:t$, and that $\eta_{st} > 0$ for the eflow. We then use Algorithm 1 to compute ebit generation ratios of the pflow corresponding to \mathcal{G}' . Let η^* be the maximally acceptable EDR of this pflow. We calculate it as $\eta^* = \min(\{f_{m:n}^{m:k}/\bar{f}_{m:n}^{m:k} \mid m, n, k \in N, \bar{f}_{m:n}^{m:k} > 0\} \cup \{g_{m:n}/\bar{g}_{m:n} \mid m, n \in N, \bar{g}_{m:n} > 0\})$. Assigning η^* to this pflow, we can update the original eflow by deducting each variable by η^* times the corresponding ebit generation ratio in the pflow. Continue this process until $\eta_{st} = 0$, and we arrive at a set of pflows with sum of EDRs equal to η_{st} . Note that in the above process, at least one $g_{m:n}$, $f_{m:n}^{m:k}$ or $f_{m:n}^{k:n}$ variable becomes 0 after updating each pflow. Since there are in total $O(N^3)$ variables, this decomposition results in at most $O(N^3)$ pflows, which is a polynomial number. \blacksquare

While it is hard for the original RED formulation in Program (6) to characterize fidelity of individual ebits generated at each enode $m:n$, we observe that each actual ebit must still be generated along a single entanglement path. Further, fidelity of the ebit is precisely defined by the underlying path along which it is generated based on Eq. (5). Assume an eflow is able to generate ebits all with fidelity no less than a given bound Υ_{st} . Following Theorem 2, the eflow can always be decomposed

into a set of sub-eflows where each eflow generates ebits along a fixed path that has fidelity lower bounded by Υ_{st} . Each sub-eflow along a path (which itself is an eflow) can further be decomposed into pflows along the same path (and thus with the same fidelity). This leads to Proposition 1 below.

Proposition 1. *An eflow with minimum end-to-end fidelity of Υ_{st} can be decomposed into a set of pflows, each representing an (s, t) -path whose fidelity is at least Υ_{st} . \square*

With Proposition 1, the design of a high-fidelity RED protocol now becomes finding an eflow that is composed of a set of pflows, each along a path with sufficiently high fidelity of the generated ebits.

D. Problem Statement

Given the decomposition theorem and Proposition 1, our goal is to find an eflow that generates high-fidelity ebits, and design a RED protocol to realize the eflow. Consider a quantum application that has an expected EDR bound Δ_{st} , and an end-to-end fidelity bound Υ_{st} for a source-destination pair.

Definition 2 (HF-RED). *Let $G = (N, L)$ be an undirected graph with node set N and link set L . Let s be a source node and t be a destination node. Let $\Delta_{st} > 0$ be an expected EDR bound and $\Upsilon_{st} > 0$ be an end-to-end fidelity bound. The **high-fidelity remote entanglement distribution** problem (denoted as HF-RED) is to seek a set of pflow, which delivers end-to-end (s, t) -ebits satisfying that*

- 1) total expected EDR η_{st} of all pflows is at least Δ_{st} , and
- 2) each pflow has fidelity no less than Υ_{st} based on Eq. (5).

For many real-world quantum applications, it is beneficial to maintain a fixed EDR, while increasing the end-to-end fidelity as much as possible, such as QKD [32]. We thus further define an optimization version of the HF-RED problem:

Definition 3 (OF-RED). *Let $G = (N, L)$ be an undirected graph with node set N and link set L . Let s be a source node and t be a destination node. Let $\Delta_{st} > 0$ be an expected entanglement distribution rate (EDR). The **optimal-fidelity remote entanglement distribution** problem (denoted as OF-RED) is to seek a set of pflow, which delivers end-to-end (s, t) -ebits satisfying that*

- 1) total expected EDR η_{st} of all pflows is at least Δ_{st} , and
- 2) the minimum end-to-end fidelity of all pflows is maximized.

E. Computational Complexity

Lemma 1. *HF/OF-RED is NP-hard. \square*

Proof: We prove NP-hardness by a reduction from the *Multi-Path routing with Bandwidth and Delay constraints (MPBD)* problem, which is NP-complete [30]. Given a graph, a source-destination pair and two values $B, D > 0$, MPBD asks for a set of paths with delay upper bounded by D , and a network flow over these paths with total flow lower bounded by B . Given an MPBD instance, let us build an instance of HF-RED. First, we set all probabilities p_l and q_n to 1. Then we set $W_l = e^{-d_l}$ where $d_l > 0$ is the delay of link l , and $W_n = 1$ for $n \in N$. Note that since $d_l > 0$, $W_l \in (0, 1)$. The fidelity bound is $\Upsilon_{st} = (1 + 3 \cdot e^{-D})/4$. Capacity c_l is set as the bandwidth in MPBD, and EDR bound $\Delta_{st} = B$. Given this construction, any ebit generated represents a path p such that $\prod_{l \in p} W_l = e^{-\sum_l d_l} \geq e^{-D}$, which gives $\sum_l d_l \leq D$.

Meanwhile, for any delay-feasible path in MPBD, generating end-to-end ebits only along this path will satisfy the fidelity bound Υ_{st} . Since entanglement generation and swapping both have success probability of 1, the EDR is exactly equal to the end-to-end (s, t) -flow value. Hence a solution to MPBD will give a feasible solution to HF-RED, and vice versa. \blacksquare

Based on the proof above, we find that the key of satisfying the fidelity constraint is to find entanglement paths with a bounded length. Let us define length values $\zeta_l = -\log(W_l)$, and $\zeta_n = -\log(W_n)$. A fidelity bound of Υ_{st} then translates to a path length bound of $Z_{st} = -\log(\frac{4\Upsilon_{st}-1}{3})$, such that $\zeta(p) = \sum_{l \in p \cap L} \zeta_l + \sum_{n \in p \cap N} \zeta_n \leq Z_{st}$ for each (s, t) -path p along which end-to-end ebits are distributed. This further transforms HF/OF-RED to finding an eflow with bounded or minimized maximum path length following Proposition 1. For clearness, we define the transformed versions of the RED problem as *bounded / optimal length RED (BL/OL-RED)*.

The NP-hardness precludes us from designing efficient yet optimal algorithms or protocols for the problem. Hence, we would like to develop approximation solutions to the problem.

Remark: For technical clarity and ease of illustration, this paper focuses on HF/OF-RED for a single source-destination pair in a quantum network. However, we note that our problem and algorithm can also be extended for high-fidelity entanglement distribution between **multiple source-destination (SD) pairs** simultaneously. Consider optimizing for the total EDR of multiple SD pairs as in most existing work [37], [47]–[49] and the *worst-case* fidelity across all SD pairs. By building an auxiliary network topology with just one artificial source and one artificial destination (connected to and from all real source nodes with an artificially perfect channel respectively), an eflow between the artificial SD pair with expected EDR η and worst-case fidelity Υ would guarantee the total expected EDR and worst-case fidelity of all actual SD pairs. Extension to other formulations, such as bounding or optimizing for the minimum instead of total EDR among SD pairs, or average instead of worst-case fidelity, is less trivial though still achievable, which we plan to design and illustrate in our future work.

V. FENDI: CONTROL PLANE ALGORITHM DESIGN

A control plane algorithm solves HF/OF-RED problem and instructs data plane operations. We design a *fully polynomial-time approximation scheme*, which achieves at most a $(1 + \varepsilon)$ factor of the optimal length, within time polynomial to $1/\varepsilon$ for arbitrary $\varepsilon > 0$. Our core idea is to find a proper quantization of the node/link lengths (equivalently the fidelity parameters), such that when solved by dynamic programming, the quantized solution approximates the optimal with controllable accuracy.

A. Maximum EDR under a Quantized Path Length Bound

We characterize a quantization of the lengths $Z = \{\zeta_i | i \in L \cup N\}$ with a factor θ , where the quantized length is denoted by $\zeta_i^\theta = \lfloor \theta \cdot \zeta_i \rfloor + 1$, for $i \in N \cup L$. Given a quantization factor θ , $Z^\theta = \{\zeta_i^\theta\}_i$ are all *positive integers*. Based on the quantized lengths, we define an extended version of Program (6).

Let Z be an *integer* path length bound given to the quantized formulation. We still keep the $g_{m:n}$ variables unchanged for $(m, n) \in L$ as in Program (6). For each $f_{m:n}^{m:k}$, we extend it into up to $O(Z^2)$ copies, denoted by $f_{m:n/z}^{m:k/z'}$, for $z' = 1, \dots, Z - \zeta_k^\theta - 1$, and $z = z' + \zeta_k^\theta + 1, \dots, Z$. In plain words,

$f_{m:n/z}^{m:k/z'}$ denotes the number of ebits between $m:k$, with a path segment length of z' , which will contribute to swapping at node k to generate ebits between $m:n$ with a path segment length of z . We similarly define $f_{m:n/z}^{k:n/z'}$ for each $f_{m:n}^{k:n}$. Both z and z' cannot exceed Z to ensure the path length bound. We then rewrite Program (6) as:

$$\max_{f,g} \quad \eta_{st}^Z = \sum_{z=1}^Z I(s, t, z) - \Omega(s, t, z) \quad (7)$$

$$\text{s.t.} \quad f_{m:n/z}^{m:k/z_1} = f_{m:n/z}^{k:n/z_2}, \forall m, n, k \in N, \\ \forall z_1, z_2 \in \{1, \dots, Z - \zeta_k^\theta - 1\}, z = z_1 + z_2 + \zeta_k^\theta; \quad (7a)$$

$$I(m, n, z) = \Omega(m, n, z), \\ \forall z \in \{1, 2, \dots, Z\}, \forall m, n \in N, \{m, n\} \neq \{s, t\}; \quad (7b)$$

where for $\forall m, n \in N, z \in \{1, 2, \dots, Z\}$,

$$I(m, n, z) \triangleq 1_{L,z}(m, n) p_{mn} c_{mn} g_{m:n} - \Omega(m, n, z) \\ + \sum_{k \in N \setminus \{m, n\}} \sum_{z'=1}^{z-\zeta_k^\theta-1} \frac{q_k}{2} \left(f_{m:n/z}^{m:k/z'} + f_{m:n/z}^{k:n/(z-z'-\zeta_k^\theta)} \right), \quad (7c)$$

$$\Omega(m, n, z) \triangleq \sum_{k \in N \setminus \{m, n\}} \left(\sum_{\substack{z'=z+1 \\ \zeta_n^\theta+1}}^Z f_{m:n/z'}^{m:k/z'} + \sum_{\substack{z'=z+1 \\ \zeta_m^\theta+1}}^Z f_{m:n/z'}^{k:n/z'} \right), \quad (7d)$$

and $1_{L,z}(m, n)$ denotes whether $(m, n) \in L$ and $\zeta_{(m,n)}^\theta = z$.

Explanation: Objective (7) is to maximize the sum of $s:t$ -ebits generated over all paths of lengths up to the bound Z . Constraint (7a) extends Constraint (6a) by considering the joint contribution to $m:n$ -ebits with a specific path length z , from a pair of $m:k$ - and $k:n$ -ebits with total path length $z - \zeta_k^\theta$. This accounts for the fact that a concatenated (m, n) -path has a total length of the (m, k) -segment and the (k, n) -segment, plus the length ζ_k^θ of node k itself. Constraint (7b) specifies flow conservation at each intermediate pair of nodes $m:n$ with each specific path length value z . The definition of $I(m, n, z)$ includes all generated ebits between m and n with a specific length z from either elementary ebit generation or intermediate swapping, minus all ebits contributed to further swapping. Overall, Program (7) has a size polynomial to the network size, and the path length bound Z .

Theorem 3. Given integer link/node lengths $\{\zeta_i^\theta\}$ for $i \in N \cup L$, and an integer length bound Z , Program (7) computes the maximum expected EDR between s and t , with all ebits generated along paths satisfying the length bound Z . \square

Proof: We call a triple $m:n/z$ by *enode* $m:n$ at level z . Let us first examine path length feasibility, i.e., ebits generated between a node pair $m:n$ at level z has path length of exactly z . For any physical link $(m, n) \in L$, the first term in Eq. (7c) ensures that $g_{m:n}$ only contributes to $I(m, n, z)$ when $z = \zeta_{(m,n)}^\theta$, i.e., elementary ebits generated along (m, n) are only counted at level $\zeta_{(m,n)}^\theta$. Then, for any triple $m:n/z$ where there exists k and z_1 such that $f_{m:n/z}^{m:k/z_1} > 0$ and $f_{m:n/z}^{k:n/z_2} > 0$ (where $z = z_1 + z_2 + \zeta_k^\theta$), we can see that if ebits at $m:k/z_1$ have path length of exactly z_1 and ebits at $k:n/z_2$ have path length of exactly z_2 , then ebits generated at $m:n/z$ by swapping them at

k exactly have path length of $z = z_1 + z_2 + \zeta_k^\theta$. By induction, any generated ebit at level z has path length of exactly z . Since there are at most Z levels, all ebits generated between $s:t$ have path lengths bounded by Z .

Next we prove optimality of Program (7). A feasible solution to Program (7) indicates a feasible solution to Program (6), by summing up the f variables and $I(\cdot)$ function values over all possible z values. Combined with path length feasibility above, the solution is feasible to quantized BL-RED. Now, for a feasible solution to quantized BL-RED, let us represent it by a set of pflows $\{\mathcal{G}\}$ with assigned values $\{\eta_{\mathcal{G}}\}$. Each $\mathcal{G} = (V, E)$ would represent a path $p_{\mathcal{G}} \in G$ with path length bounded by Z . We can construct a feasible solution to Program (7) given each \mathcal{G} . For each enode $m:n \in \mathcal{G}$, let $\zeta_{m:n}^\theta$ be the quantized length of the path segment in G between m and n that is represented by \mathcal{G} (which can be computed for each $m:n$ in linear time). For each enode $m:n \in V$ that has no in-coming link, we set $g_{m:n} = \bar{g}_{m:n} \cdot \eta_{\mathcal{G}}$. Then, for each $(m:k, m:n) \in E$, we set $f_{m:n/\zeta_{m:n}^\theta}^{m:k/\zeta_{m:n}^\theta} = f_{m:n/\zeta_{m:n}^\theta}^{k:n/\zeta_{m:n}^\theta} = \bar{f}_{m:n}^{m:k} \cdot \eta_{\mathcal{G}}$. It can be checked that the constructed solution is feasible to Program (7) based on how $\{\bar{g}_{m:n}, \bar{f}_{m:n}^{m:k}, \bar{f}_{m:n}^{k:n}\}$ are computed, how \mathcal{G} is defined, and that each \mathcal{G} represents a path with length bounded by Z . Summing up so-constructed solutions for all of $\{\mathcal{G}\}$ and $\{\eta_{\mathcal{G}}\}$, we get a feasible solution to Program (7), with the same objective value $\eta_{st}^Z = \sum_{\mathcal{G}} \eta_{\mathcal{G}}$. It follows that Program (7) outputs the maximum expected EDR among all feasible eflows that satisfy the path length bound of Z . \blacksquare

Proposition 2. Program (7) can be solved optimally, in time polynomial to the input size and Z . \square

Proof: Program (7) is an LP with $O(|N|^3 Z^2)$ variables, and can be solved in time polynomial to $|N|$ and Z [44]. \blacksquare

B. An Approximate Testing Procedure

Program (7) provides a pseudo-polynomial time solution to the quantized BL-RED (QBL-RED) problem, which can be used to check if an instance of QBL-RED has a feasible solution: if the computed maximum EDR cannot meet EDR bound Δ_{st} , the QBL-RED instance is infeasible, and vice versa. We leverage this to design an *approximate testing* procedure, which serves as a crucial building block of our final solution design.

Let $\zeta^\theta(p)$ be the length of an arbitrary path p in G after quantization with factor θ , and recall that $\zeta(p)$ is the original path length. We have the following lemma:

Lemma 2. $\theta \cdot \zeta(p) \leq \zeta^\theta(p) \leq \lceil \theta \cdot \zeta(p) \rceil + (2|N| - 3)$. \square

Proof: The left side is trivial due to how lengths are quantized. The right side is because 1) each entanglement path in G has at most $|N|-1$ links and $|N|-2$ intermediate nodes whose lengths are counted (excluding source and destination), and 2) $\zeta^\theta(p)$ is an integer value due to quantization (and hence the floor over $\theta \cdot \zeta(p)$ on the right side). \blacksquare

Algorithm 2: Approximate testing procedure TEST(Z, ε)

Input: Network G , accuracy ε , non-quantized length bound Z

Output: Test result $\varsigma \in \{true, false\}$

- 1 $\theta \leftarrow (2|N| - 3)/(\varepsilon Z)$, and $Z \leftarrow \lfloor \theta Z \rfloor + (2|N| - 3)$;
 - 2 Solve Program (7) with θ and Z , and get η_{st}^Z ;
 - 3 **return** ((Program (7) is feasible) AND ($\eta_{st}^Z \geq \Delta_{st}$)).
-

Based on Lemma 2, we design the approximate testing procedure in Algorithm 2. The algorithm returns a test result $\varsigma \in \{true, false\}$, which indicates whether given ε and a non-quantized length bound \mathbf{Z} , the QBL-RED instance with quantization factor θ and quantized length bound Z as in Line 1 admits a feasible solution. Let \mathbf{Z}^* be the optimal solution of the original OL-RED instance before quantization. Lemma 3 shows why this testing procedure is useful:

Lemma 3. *Given any $\varepsilon > 0$ and $\mathbf{Z} > 0$, we have*

$$\begin{aligned} \text{TEST}(\mathbf{Z}, \varepsilon) = \text{true} &\Rightarrow \mathbf{Z}^* \leq (1 + \varepsilon) \cdot \mathbf{Z}; \\ \text{TEST}(\mathbf{Z}, \varepsilon) = \text{false} &\Rightarrow \mathbf{Z}^* > \mathbf{Z}. \end{aligned} \quad \square$$

Proof: If $\text{TEST}(\mathbf{Z}, \varepsilon) = \text{true}$, the QBL-RED instance is feasible with $\eta_{st}^Z \geq \Delta_{st}$ and all paths satisfying bound Z . This translates to a feasible solution to OL-RED with EDR bound Δ_{st} . Let p be the maximum-length path in the solution w.r.t. the original lengths \mathcal{Z} . Following Lemma 2, we have:

$$\zeta(p) \leq \zeta^\theta(p)/\theta \leq Z/\theta \leq (1 + \varepsilon)\mathbf{Z}.$$

Since the solution is feasible to OL-RED, its maximum (non-quantized) path length is an upper bound on \mathbf{Z}^* , and hence we have $\mathbf{Z}^* \leq (1 + \varepsilon)\mathbf{Z}$. This proves the first statement.

To prove the second statement, we show that as long as there is a feasible OL-RED solution which has maximum path length bounded by \mathbf{Z} , then $\text{TEST}(\mathbf{Z}, \varepsilon)$ must return *true*. Consider such a solution and let its maximum path length be $\mathbf{Z}' \leq \mathbf{Z}$. By Lemma 2, we have:

$$\zeta^\theta(p) \leq \theta \cdot \zeta(p) + (2|N| - 3) \leq (2|N| - 3)/\varepsilon + (2|N| - 3).$$

Since $\zeta^\theta(p)$ must be an integer, this implies $\zeta^\theta(p) \leq \lfloor (2|N| - 3)/\varepsilon \rfloor + (2|N| - 3) = \lfloor \theta \mathbf{Z} \rfloor + (2|N| - 3) = Z$. By Theorem 3, this solution can be decomposed into a set of pflows, whose maximum quantized path length is $\zeta^\theta(p)$, and whose sum of objective values equals $\eta_{st}^Z \geq \Delta_{st}$. In this case, $\text{TEST}(\mathbf{Z}, \varepsilon)$ must return *true*. Hence if $\text{TEST}(\mathbf{Z}, \varepsilon)$ returns *false*, it indicates there is no such feasible solution. ■

C. A Fully Polynomial-Time Approximation Scheme

With the testing procedure in Algorithm 2, we now design a *fully polynomial time approximation scheme (FPTAS)* for the OL-RED problem (and also for OF-RED as shown later in Corollary 1). Our first step is to find a pair of bounds (LB, UB) on \mathbf{Z}^* , such that $\text{LB} \leq \mathbf{Z}^* \leq \text{UB}$, as shown in Algorithm 3.

Algorithm 3: Finding lower and upper bounds on \mathbf{Z}^*

Input: Network G

Output: Lower and upper bounds (LB, UB) on \mathbf{Z}^*

- 1 Sort node/link lengths in $\{\zeta_l \mid l \in L\} \cup \{\zeta_n \mid n \in N\}$ in descending order as $\mathcal{Z} = (\zeta_{[1]}, \zeta_{[2]}, \dots)$;
 - 2 **for** $\zeta_{[i]} \in \mathcal{Z}$ **in sorted order do**
 - 3 Construct graph $G_{[i]}$ by pruning all nodes and links with lengths greater than $\zeta_{[i]}$ in G ;
 - 4 Solve Program (6) on $G_{[i]}$ for $\eta_{st}^{[i]}$;
 - 5 **if** *Infeasible* or $\eta_{st}^{[i]} < \Delta_{st}$ **then break**;
 - 6 **return** $(\text{LB} = \zeta_{[i-1]}, \text{UB} = (2|N| - 3)\zeta_{[i-1]})$.
-

Algorithm 3 sorts all node/link lengths in descending order, and then tries to find a *critical length* $\zeta_{[i-1]}$ such that $G_{[i-1]}$ still admits a feasible solution to Program (6) with $\eta_{st}^{[i-1]} \geq \Delta_{st}$, but $G_{[i]}$ does not. This means at least one node/link with length no less than $\zeta_{[i-1]}$ is needed to satisfy the EDR bound of Δ_{st} . Consequently, the optimal \mathbf{Z}^* must be at least $\zeta_{[i-1]}$

Algorithm 4: 2-stage Bisection for Approximate OL-RED

Input: Network G , search accuracy parameter ε

Output: Eflow with maximum path length \mathbf{Z}^+

- 1 Call Algorithm 3 to find LB and UB on \mathbf{Z}^* ;
 - 2 **while** $\text{UB} > 4 \cdot \text{LB}$ **do** // Stage-1
 - 3 $\mathbf{Z} = \sqrt{(\text{UB} \cdot \text{LB})/2}$;
 - 4 **if** $\text{TEST}(\mathbf{Z}, 1) = \text{false}$ **then** $\text{LB} \leftarrow \mathbf{Z}$;
 - 5 **else** $\text{UB} \leftarrow 2 \cdot \mathbf{Z}$;
 - 6 $\theta \leftarrow \frac{2|N|-3}{\varepsilon \text{LB}}$, $Z_{\text{LB}} \leftarrow \lfloor \theta \text{LB} \rfloor$, $Z_{\text{UB}} \leftarrow \lfloor \theta \text{UB} \rfloor + (2|N| - 3)$;
 - 7 **while** $Z_{\text{UB}} > Z_{\text{LB}} + 1$ **do** // Stage-2
 - 8 $Z \leftarrow \lfloor (Z_{\text{LB}} + Z_{\text{UB}})/2 \rfloor$;
 - 9 Solve Program (7) with θ and Z , and get η_{st}^Z ;
 - 10 **if** Program (7) is feasible AND $\eta_{st}^Z \geq \Delta_{st}$ **then**
 - 11 $Z_{\text{UB}} \leftarrow Z$;
 - 11 **else** $Z_{\text{LB}} \leftarrow Z$;
 - 12 **return** last feasible solution with max path length \mathbf{Z}^+
-

as a lower bound. Besides, since there is a feasible solution in $G_{[i-1]}$, and each path can have at most $|N| - 1$ links and $|N| - 2$ intermediate nodes, the feasible solution has a maximum path length of $(2|N| - 3) \cdot \zeta_{[i-1]}$ as all nodes and links in $G_{[i-1]}$ have lengths at most $\zeta_{[i-1]}$. This shows that $(2|N| - 3) \cdot \zeta_{[i-1]}$ is an upper bound on \mathbf{Z}^* .

With (LB, UB) found by Algorithm 3, we can apply a bisection search on the range $[\text{LB}, \text{UB}]$ to find an approximator of \mathbf{Z}^* . Each time we define a bound $\mathbf{Z} = (\text{LB} + \text{UB})/2$, and call $\text{TEST}(\mathbf{Z}, \varepsilon)$. If $\text{TEST}(\mathbf{Z}, \varepsilon)$ outputs *true*, we narrow the gap by setting $\text{UB} \leftarrow (1 + \varepsilon)\mathbf{Z}$; otherwise, we set $\text{LB} \leftarrow \mathbf{Z}$. To achieve an arbitrary accuracy, it takes $O(\log(\text{UB} - \text{LB})) = O(\log(|N| \zeta_{\max}))$ search iterations (where ζ_{\max} is the maximum length value in the graph), each making a call to $\text{TEST}(\mathbf{Z}, \varepsilon)$ which solves an LP of size $O\left(|N|^3 \left(\frac{|N|}{\varepsilon}\right)^2\right)$.

In Algorithm 4, we propose an improved *2-stage search algorithm*, which reduces the asymptotic search complexity and sizes of the LPs solved in most search iterations. In Stage-1 (Lines 2–5), a *multiplicative bisection* (bisection in the logarithm scale) is done on (LB, UB), where each time an $\varepsilon = 1$ is used in approximate testing. By Lemma 3, $\text{TEST}(\mathbf{Z}, 1)$ returning *false* means $\mathbf{Z}^* > \mathbf{Z}$ and hence LB is increased to \mathbf{Z} ; $\text{TEST}(\mathbf{Z}, 1)$ returning *true* means $\mathbf{Z}^* \leq (1 + \varepsilon) \cdot \mathbf{Z} = 2\mathbf{Z}$ and hence UB is decreased to $2\mathbf{Z}$. Stage-1 ends when LB and UB are within a constant factor of each other, such as 4.

In Stage-2, instead of doing bisection directly on [LB, UB], we do a bisection on the quantized bounds $[Z_{\text{LB}}, Z_{\text{UB}}]$. We fix the quantization factor $\theta = (2|N| - 3)/(\varepsilon \text{LB})$, and only vary the quantized path length bound Z . The main purpose of this construction is to utilize quantization to naturally reduce the number of search iterations to achieve the desired accuracy defined by ε . Since LB and UB are within a constant ratio of each other, the quantized length bound $Z_{\text{UB}} \in O(|N|/\varepsilon)$, and hence $O(\log(|N|/\varepsilon))$ search iterations are needed to search all integers between Z_{LB} and Z_{UB} . This makes the search complexity no longer related to ζ_{\max} as in the naive bisection search. Let \mathbf{Z}^θ be the optimal maximum path length for *quantized OL-RED (QOL-RED)* with θ . The following lemmas show that this quantized bisection is as effective as the bisection search on the original bounds [LB, UB].

Lemma 4. $\lfloor \theta \text{LB} \rfloor \leq \mathbf{Z}^\theta \leq \lfloor \theta \text{UB} \rfloor + (2|N| - 3)$. □

Lemma 5. $\mathbf{Z}^\theta \leq \theta \cdot (1 + \varepsilon) \cdot \mathbf{Z}^*$. □

Proof: Note that a feasible solution to original OL-RED indicates a feasible solution to QOL-RED, and vice versa. Given the optimal solution to original OL-RED with objective \mathbf{Z}^* , let p be its longest entanglement path such that $\zeta(p) = \mathbf{Z}^*$, and let p_θ be its longest entanglement path with quantization. By Lemma 2, $\zeta^\theta(p_\theta) \leq \lfloor \theta \zeta(p_\theta) \rfloor + (2|N| - 3) \leq \lfloor \theta \zeta(p) \rfloor + (2|N| - 3) \leq \lfloor \theta \mathbf{UB} \rfloor + (2|N| - 3)$. This proves the right-hand side of Lemma 4, as \mathbf{Z}^θ is optimal and hence $\mathbf{Z}^\theta \leq \zeta^\theta(p_\theta)$. Further, since $\zeta(p) = \mathbf{Z}^*$, we have $\zeta^\theta(p_\theta) \leq \theta \zeta(p) + (2|N| - 3) = \theta(\mathbf{Z}^* + (2|N| - 3)/\theta) = \theta(\mathbf{Z}^* + \varepsilon \mathbf{LB}) \leq \theta \cdot (1 + \varepsilon) \cdot \mathbf{Z}^*$, and hence $\mathbf{Z}^\theta \leq \zeta^\theta(p_\theta) \leq \theta \cdot (1 + \varepsilon) \cdot \mathbf{Z}^*$, proving Lemma 5.

Now consider the optimal solution to QOL-RED, and let p'_θ be its quantized longest entanglement path, where $\zeta^\theta(p'_\theta) = \mathbf{Z}^\theta$. Also let p' be its longest entanglement path without quantization. Since this solution is also feasible to OL-RED, we have $\theta \mathbf{LB} \leq \theta \mathbf{Z}^* \leq \theta \zeta(p')$. By Lemma 2, we then have $\theta \zeta(p') \leq \zeta^\theta(p') \leq \zeta^\theta(p'_\theta) = \mathbf{Z}^\theta$. Hence $\mathbf{Z}^\theta \geq \lfloor \theta \mathbf{LB} \rfloor$. ■

Theorem 4. *Given accuracy parameter ε , Algorithm 4 find a $(1 + \varepsilon)$ -approximation of the optimal OL-RED objective value \mathbf{Z}^* , within time polynomial to $|N|$ and $1/\varepsilon$.* □

Proof: The approximation ratio directly comes from Lemma 5. Let $T(x)$ be the worst-case time for solving an LP with x variables. First, calling Algorithm 3 to find a pair of bounds (LB, UB) on \mathbf{Z}^* takes up to $|\mathcal{Z}| = |N| + |L|$ iterations, each solving Program (6) with $O(|N|^3)$ variables in $O(T(|N|^3))$ time. For the Stage-1 bisection, let $\pi_{[j]}$ be the ratio UB/LB after the j -th iteration. Initially $\pi_{[0]} = 2|N| - 3$ due to the (LB, UB) bound by Algorithm 3. After each iteration $j \geq 1$, $\pi_{[j]} = \sqrt{2\pi_{[j-1]}}$ based on how \mathbf{Z} is computed. Let J be index of the last iteration, and applying the above recursively, we have $\pi_{[J]} = 2^{1/2+1/4+\dots+1/2^J} \cdot \pi_{[0]}^{1/2^J} \leq 2 \cdot \pi_{[0]}^{1/2^J} = 2 \cdot (2|N| - 3)^{1/2^J}$. As $\pi_{[J]} \leq 4$ in the ending condition of Stage-1, the total number of iterations is $O(\log \log |N|)$. Each iteration solves Program (7) with $\varepsilon = 1$, and hence $Z \in O(|N|)$, which results in the program having $O(|N|^3 Z^2) = O(|N|^5)$ variables, and hence each iteration takes $O(T(|N|^5))$ time. For Stage-2, the bisection is performed on up to $Z_{\text{UB}} \in O(\frac{|N|}{\varepsilon})$ integers, with up to $O(\log \frac{|N|}{\varepsilon})$ search iterations. Each iteration solves Program (7) with $O(|N|^3 Z_{\text{UB}}^2) = O(\frac{|N|^5}{\varepsilon^2})$ variables, and hence each iteration takes $O(T(\frac{|N|^5}{\varepsilon^2}))$ time. Summing up the above, the overall time complexity is $O(T(|N|^3) \cdot (|N| + |L|) + T(|N|^5) \cdot \log \log |N| + T(|N|^5/\varepsilon^2) \cdot \log \frac{|N|}{\varepsilon})$. Given that an LP can be solved in polynomial time [44], the above time is polynomial to $|N|$ and $1/\varepsilon$. ■

Corollary 1. *Given fidelity accuracy parameter $\omega \in (0, 1)$, let $\varepsilon = -(\ln(1 - \omega))/\mathbf{UB}$. The minimum fidelity of ebits generated by a solution output by Algorithm 4 is lower bounded by $(1 - \omega)$ times the optimal minimum fidelity, i.e., the solution is a $(1 - \omega)$ -approximation to OF-RED.* □

Proof: Recall that a path p with length $\zeta(p)$ has fidelity parameter of $W_p = e^{-\zeta(p)}$ (as in Sec. IV) and fidelity of $F_p = (1 + 3W_p)/4$ (as in Eq. (5)). Let W^* and F^* be the optimal fidelity parameter and optimal fidelity of any feasible eflow to OF-RED, and let W^+ and F^+ be fidelity parameter and fidelity of the solution output by Algorithm 4. Given $\varepsilon > 0$, Algorithm 4 outputs a solution with $\mathbf{Z}^+ \leq (1 + \varepsilon) \cdot \mathbf{Z}^*$, which means $W^+ = e^{-\mathbf{Z}^+} \geq e^{-(1+\varepsilon)\mathbf{Z}^*} = (W^*)^{(1+\varepsilon)} = W^* \cdot (W^*)^{-(\ln(1-\omega))/\mathbf{UB}} \geq W^* \cdot (W^*)^{-(\ln(1-\omega))/\mathbf{Z}^*} = W^*$.

$(W^*)^{(\ln(1-\omega))/\ln(W^*)} = (1 - \omega)W^*$. Therefore, $F^+ = (1 + 3W^+)/4 \geq (1 + 3(1 - \omega)W^*)/4 \geq (1 - \omega)(1 + 3W^*)/4 \geq (1 - \omega)F^*$, proving the corollary. To sum up, Algorithm 4 where ε is set given ω and after obtaining UB in Line 1 gives us an FPTAS to OF-RED. ■

Remark: Despite being polynomial-time, Algorithm 4 still has high complexity due to solving the large-size LPs. There are several methods to reduce running time: 1) setting a loose ε or ω , which is commonly over-conservative for practical settings; 2) applying heuristic quantization rules that work empirically; 3) developing heuristic algorithms to solve the quantized LP. We will examine effect of the first method in our evaluation. Considering that the quantum network is designed for long-term operations, the overhead of offline optimization can often be negligible. For instance, by spending minutes or hours to compute a high-EDR and high-fidelity RED plan for a QKD application [32], the resulting plan could be executed and deliver significantly improved performance over a period of weeks or months before offline maintenance/re-optimization is needed. We will explore efficient real-time RED protocol design, including along the above lines, in our future research.

VI. FENDI: DATA PLANE PROTOCOL DESIGN

Given a solution output by a central quantum network controller running Algorithm 4, we design an extension of the protocol in [14] to achieve the expected EDR and guarantee that all generated ebits have end-to-end fidelity of at least Υ_{st} .

Specifically, after the computation, the quantization θ and the final quantized path length bound Z_{UB} are distributed to each quantum repeater along with the solution. For every enode $m:n$, both nodes maintain **input buffers** $\mathcal{E}_{m:n/z}$ for every value $z = 1, 2, \dots, Z_{\text{UB}}$. $\mathcal{E}_{m:n/z}$ stores the ebits generated between $m:n$ with a specific range of fidelity values represented by a quantized length z . They also maintain **output buffers** $\mathcal{D}_{m:n/z}^{m:k/z'}$ and $\mathcal{D}_{k:n/z'}^{m:n/z}$ respectively for every $k \neq m, n$ and $z' > z$, which stores the ebits that will be contributed to generating ebits between other pairs with other fidelity values. Note that the number and sizes of buffers at each node may be dynamically adjusted by allocating the available quantum memories, based on f and g variables that have positive values, i.e., the corresponding enodes that are expecting ebits.

To execute the protocol, each link $(m, n) \in E$ will continuously generate $c_{mn} \cdot g_{m:n}$ elementary ebits. Once successfully generated, these ebits are added to the buffer $\mathcal{E}_{m:n/z}$ where $z = \zeta_{(m,n)}^\theta = \lfloor -\log(W_{mn})\theta \rfloor + 1$. Simultaneously, whenever an ebit is added to $\mathcal{E}_{m:n/z}$ for any z , the two end points will jointly toss a random coin, and move the ebit from $\mathcal{E}_{m:n/z}$ to $\mathcal{D}_{m:k/z'}^{m:n/z}$ or $\mathcal{D}_{k:n/z'}^{m:n/z}$ with the following probabilities:

$$\Pr[\text{move to } \mathcal{D}_{m:k/z'}^{m:n/z}] = \frac{f_{m:k/z'}^{m:n/z}}{\sum_{z''} \sum_k (f_{m:k/z''}^{m:n/z} + f_{k:n/z''}^{m:n/z})};$$

$$\Pr[\text{move to } \mathcal{D}_{k:n/z'}^{m:n/z}] = \frac{f_{k:n/z'}^{m:n/z}}{\sum_{z''} \sum_k (f_{m:k/z''}^{m:n/z} + f_{k:n/z''}^{m:n/z})}.$$

Finally, each node k will be checking if for any $m:n$, there exists z_1, z_2, z_3 such that

- 1) $z_1 + z_2 + \zeta_k^\theta = z_3$;
- 2) $f_{m:k/z_1}^{m:n/z_3} = f_{m:n/z_3}^{k:n/z_2} > 0$; and
- 3) $\mathcal{D}_{m:n/z_3}^{m:k/z_1} \neq \emptyset$, and $\mathcal{D}_{m:n/z_3}^{k:n/z_2} \neq \emptyset$.

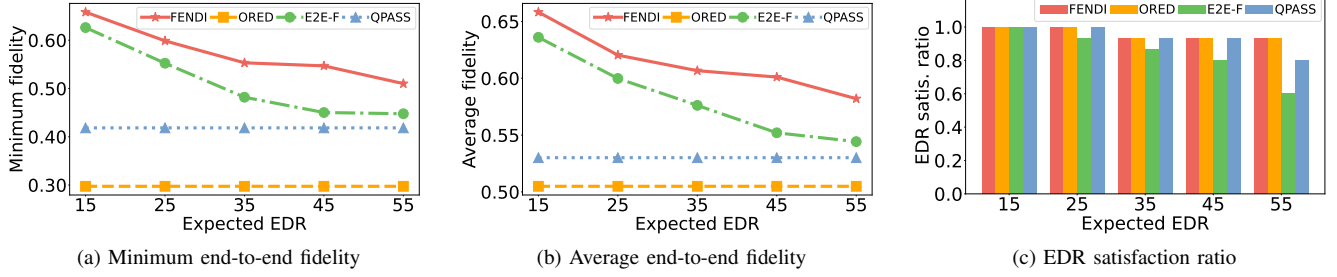


Fig. 3: Comparison between FENDI and state-of-the-art algorithms

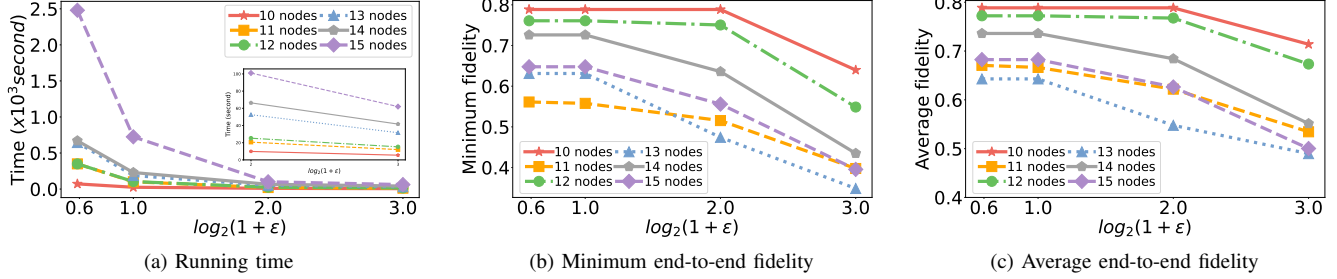


Fig. 4: Performance and running time of FENDI with varying ϵ and number of nodes

For each such a case, node k locally performs swapping between each pair of ebits in $\mathcal{D}_{m:n/z_1}^{m:k/z_1}$ and $\mathcal{D}_{m:n/z_2}^{k:n/z_2}$ respectively. Upon success, the ebit will then be added to $\mathcal{E}_{m:n/z_3}^{m:n/z_3}$ by m and n . The source and destination will keep all ebits received in $\mathcal{E}_{s:t/z}$ for any z . All the above processes can be parallel and asynchronous. The strong network-wide synchronization requirement in traditional time-slotted entanglement routing protocols is thus relaxed. By an induction proof similar to the one in [14] which we omit due to page limit, this protocol is guaranteed to achieve a long-term EDR of at least Δ_{st} and an end-to-end fidelity of at least Υ_{st} , which is at least $(1-\omega)$ times the optimal fidelity to support this long-term EDR.

VII. PERFORMANCE EVALUATION

A. Evaluation Methodology

To evaluate our solution, we developed a discrete-time quantum network simulator. We used random Waxman graphs [43] with parameters $\alpha = \beta = 0.8$. Each node or link had a success probability of 0.9, and fidelity uniformly sampled from $[0.7, 0.95]$. Each link had a capacity uniformly sampled from $[26, 35]$. Parameters are selected as the same value as in the previous work [49]. In each setting, we generated 5 graphs each with 3 random source-destination pairs. Results were averaged over all runs in the same setting to average-out random noise.

Our simulator was based on a time-slotted model to be compatible to existing algorithms, even though our data plane does not require network-wide synchronization. We implemented our control plane algorithm as well as several state-of-the-arts. Linear programs were solved using the Gurobi solver [1]. Simulations were ran on a Linux desktop with a 12-core 4GHz CPU and 256GB memory. In each simulation, we first ran a control plane algorithm for the picked source-destination pair. Based on the solution, we then simulated entanglement

generation, swapping and/or queuing for 1000 time slots. The following control plane algorithms were compared:

- **FENDI**: Our proposed algorithm in Algorithm 4.
- **ORED**: The fidelity-agnostic ORED algorithm in [14].
- **E2E-F**: End-to-end fidelity-aware entanglement routing in [49], *without purification* for fair comparison.
- **QPASS**: Fidelity-agnostic entanglement routing in [37].

For our algorithm, we set $\epsilon = 0.5$ by default. For QPASS and E2E-F, we set the number of paths $K = 15$. Since E2E-F and QPASS are *entanglement routing* algorithms for a bufferless quantum network, we adapted our simulator to discard all saved ebits after one time slot when simulating them.

The following metrics were used for evaluation. The **minimum fidelity** and **average fidelity** respectively measure the lowest and average fidelity values of all end-to-end entanglements generated following a control plane algorithm. The **EDR satisfaction ratio** measures the fraction of simulation runs where the EDR bound is met. The **running time** measures the average time spent on running each *control plane* algorithm.

B. Evaluation Results

1) *Comparison with state-of-the-arts*: Fig. 3 shows the comparison results between FENDI and other algorithms, with varying expected EDR bounds. From Figs. 3(a)–(b), FENDI achieved the highest fidelity compared to all other algorithms. The two fidelity-aware algorithms (FENDI and E2E-F) achieved significantly higher fidelity than the fidelity-agnostic algorithms (ORED and QPASS), demonstrating the *crucial need for fidelity awareness in quantum networking*. With increasing EDR bounds, fidelity-aware algorithms traded-off fidelity to meet the EDR requirement, by utilizing paths with lower fidelity. The fidelity gap between FENDI and E2E-F generally increased with higher EDR bounds, demonstrating *importance of our approximation guarantee*. Note that for many applications such as entanglement purification [3], entanglements are regarded as non-usable when fidelity drops below 0.5. Fig. 3(a) shows that to ensure minimum fidelity over

0.5, our algorithm can achieve significantly higher expected EDR, even compared to existing fidelity-aware algorithm such as E2E-F.

From Fig. 3(c), FENDI achieved EDR satisfaction ratios on par with ORED. This is because both algorithms explore the same EDR feasibility region, and differ only by fidelity of paths (pflows) to meet a given expected EDR bound. Both FENDI and ORED achieved higher EDR satisfaction ratio than QPASS and E2E-F, even though E2E-F achieved similar (but still lower) fidelity compared to FENDI and higher fidelity than ORED. There are two reasons: 1) FENDI and ORED are *optimal* in terms of whether an expected EDR bound can be satisfied while E2E-F and QPASS have no such guarantee; 2) *a buffered quantum network can achieve higher long-term EDR than a bufferless network by storing instead of discarding unused intermediate ebits.*

2) *Performance versus running time:* Fig. 4 shows the evaluation result for the trade-off between performance and running time for FENDI, with varying number of nodes and accuracy parameter ε . Note that despite ε , FENDI always achieved the same EDR satisfaction ratio as the same feasibility region of the problem was explored, and thus we omit the figure showing the EDR satisfaction ratio. From Fig. 4(a), the running time increased with number of nodes and decreased with ε . From Figs. 4(b) and 4(c), increasing ε led to fidelity reduction, matching our theoretical analysis. However, with a relatively loose ε , such as when $\varepsilon = 1$ or 3, the achieved fidelity was on par with when ε was set to a tight value such as 0.5. This shows that the theoretical guarantee tends to be over-conservative in practice, and *it is reasonable to set a loose ε value to achieve high time efficiency with reasonable performance.* The correlation between number of nodes and fidelity values of FENDI was weak. This could be because, on one hand, a larger graph with more nodes could lead to more paths between each source-destination pair and hence increase fidelity; on the other hand, a larger graph also means it is more likely that two randomly picked nodes are further away in the graph, leading to degraded fidelity over long paths. The potential trade-off between network size and fidelity will be explored in our future work, possibly on larger network topologies with more scalable algorithms.

VIII. CONCLUSIONS

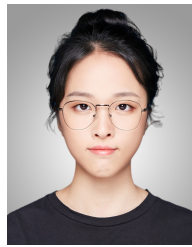
In this paper, we proposed FENDI, a *high-fidelity remote entanglement distribution (HF-RED)* algorithm coupled with a data plane protocol for buffered quantum networks with theoretical guarantee. We derived an end-to-end fidelity model for worst-case (isotropic) noise. We then formulated the HF-RED problem and proved its NP-hardness. Utilizing a novel decomposition theorem, we developed a *fully polynomial-time approximation scheme (FPTAS)* for the problem, and a data plane protocol that implemented the solution of the FPTAS. We developed a discrete-time quantum network simulator for evaluation. Extensive simulation results showed the superior performance of FENDI, compared to existing entanglement routing and distribution algorithms.

REFERENCES

- [1] “Gurobi Optimizer,” accessed 2022-07-25. URL: <http://www.gurobi.com/products/gurobi-optimizer>
- [2] M. F. Askarani, K. Chakraborty, and G. C. Do Amaral, “Entanglement distribution in multi-platform buffered-router-assisted frequency-multiplexed automated repeater chains,” *New Journal of Physics*, vol. 23, no. 6, p. 063078, 2021.
- [3] C. H. Bennett, H. J. Bernstein, S. Popescu, and B. Schumacher, “Concentrating partial entanglement by local operations,” *Physical Review A*, vol. 53, no. 4, p. 2046, 1996.
- [4] C. H. Bennett and G. Brassard, “Quantum cryptography: Public key distribution and coin tossing,” *Theoretical Computer Science*, vol. 560, pp. 7–11, 2014.
- [5] C. H. Bennett, D. P. DiVincenzo, J. A. Smolin, and W. K. Wootters, “Mixed-state entanglement and quantum error correction,” *Physical Review A*, vol. 54, no. 5, p. 3824, 1996.
- [6] A. S. Cacciapuoti, M. Caleffi, F. Tafuri, F. S. Cataliotti, S. Gherardini, and G. Bianchi, “Quantum Internet: Networking challenges in distributed quantum computing,” *IEEE Network*, vol. 34, no. 1, pp. 137–143, 2019.
- [7] M. Caleffi, “Optimal routing for quantum networks,” *IEEE Access*, vol. 5, pp. 22 299–22 312, 2017.
- [8] M. Caleffi, A. S. Cacciapuoti, and G. Bianchi, “Quantum Internet: From communication to distributed computing!” in *ACM NANOCOM*, 2018, pp. 1–4.
- [9] K. Chakraborty, F. Rozpedek, A. Dahlberg, and S. Wehner, “Distributed routing in a quantum internet,” *arXiv preprint arXiv:1907.11630*, 2019.
- [10] A. Chang and G. Xue, “Order matters: On the impact of swapping order on an entanglement path in a quantum network,” in *IEEE INFOCOM WKSHPS*, 2022, pp. 1–6.
- [11] L. Chen, Q. Chen, M. Zhao, J. Chen, S. Liu, and Y. Zhao, “DDKA-QKDN: Dynamic on-demand key allocation scheme for quantum internet of things secured by qkd network,” *Entropy*, vol. 24, no. 2, p. 149, 2022.
- [12] C. Cicconetti, M. Conti, and A. Passarella, “Resource allocation in quantum networks for distributed quantum computing,” *arXiv preprint arXiv:2203.05844*, 2022.
- [13] A. Dahlberg, M. Skrzypczyk, T. Coopmans, L. Wubben, F. Rozpedek, M. Pompili, A. Stolk, P. Pawelczak, R. Knegjens, J. de Oliveira Filho *et al.*, “A link layer protocol for quantum networks,” in *ACM SIGCOMM*, 2019, pp. 159–173.
- [14] W. Dai, T. Peng, and M. Z. Win, “Optimal protocols for remote entanglement distribution,” in *IEEE ICNC*, 2020, pp. 1014–1019.
- [15] —, “Optimal remote entanglement distribution,” *IEEE Journal on Selected Areas in Communications*, vol. 38, no. 3, pp. 540–556, 2020.
- [16] —, “Quantum queuing delay,” *IEEE Journal on Selected Areas in Communications*, vol. 38, no. 3, pp. 605–618, 2020.
- [17] S. Das, S. Khatri, and J. P. Dowling, “Robust quantum network architectures and topologies for entanglement distribution,” *Physical Review A*, vol. 97, no. 1, p. 012335, 2018.
- [18] S. DiAdamo, B. Qi, G. Miller, R. Kompella, and A. Shabani, “Packet switching in quantum networks: A path to quantum internet,” *arXiv preprint arXiv:2205.07507*, 2022.
- [19] Y. Dudin, L. Li, and A. Kuzmich, “Light storage on the time scale of a minute,” *Physical Review A*, vol. 87, no. 3, p. 031801, 2013.
- [20] W. Dür, H.-J. Briegel, J. I. Cirac, and P. Zoller, “Quantum repeaters based on entanglement purification,” *Physical Review A*, vol. 59, pp. 169–181, Jan 1999.
- [21] C. Elliott, “Building the quantum network,” *New Journal of Physics*, vol. 4, no. 1, p. 46, 2002.
- [22] R. P. Feynman, “Simulating physics with computers,” *International Journal of Theoretical Physics*, vol. 21, no. 6/7, 1982.
- [23] L. Kleinrock, “Information flow in large communication nets,” *RLE Quarterly Progress Report*, vol. 1, 1961.
- [24] —, *Queueing Systems. Volume II: Computer Applications*. Wiley, 1976.
- [25] M. Koashi and N. Imoto, “No-cloning theorem of entangled states,” *Physical Review Letters*, vol. 81, no. 19, p. 4264, 1998.
- [26] W. Kozłowski, A. Dahlberg, and S. Wehner, “Designing a quantum network protocol,” in *ACM CoNEXT*, 2020, pp. 1–16.
- [27] N. Leslie, J. Devin, and T. W. Lynn, “Maximal l1-norm distinguishability

of qubit and qutrit bell states using projective and non-projective measurements,” *Quantum Physics*, 2019.

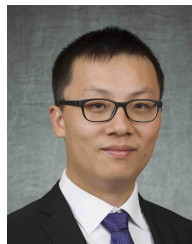
- [28] J. Li, Q. Jia, K. Xue, D. S. L. Wei, and N. Yu, “A connection-oriented entanglement distribution design in quantum networks,” *IEEE Transactions on Quantum Engineering*, vol. 3, pp. 1–13, 2022.
- [29] Y. Ma, Y.-Z. Ma, Z.-Q. Zhou, C.-F. Li, and G.-C. Guo, “One-hour coherent optical storage in an atomic frequency comb memory,” *Nature Communications*, vol. 12, no. 1, pp. 1–6, 2021.
- [30] S. Misra, G. Xue, and D. Yang, “Polynomial time approximations for multi-path routing with bandwidth and delay constraints,” in *IEEE INFOCOM*, 2009, pp. 558–566.
- [31] M. Pant, H. Krovi, D. Towsley, L. Tassiulas, L. Jiang, P. Basu, D. Englund, and S. Guha, “Routing entanglement in the quantum internet,” *npj Quantum Information*, vol. 5, no. 1, pp. 1–9, 2019.
- [32] M. Peev, C. Pacher, R. Alléaume, C. Barreiro, J. Bouda, W. Boxleitner, T. Debuisschert, E. Diamanti, M. Dianati, J. Dynes *et al.*, “The secoqc quantum key distribution network in vienna,” *New Journal of Physics*, vol. 11, no. 7, p. 075001, 2009.
- [33] S. Pouryousef, N. K. Panigrahy, and D. Towsley, “A quantum overlay network for efficient entanglement distribution,” *arXiv preprint arXiv:2212.01694*, 2022.
- [34] S. I. Salim, A. Quaium, S. Chellappan, and A. B. M. A. Al Islam, “Enhancing fidelity of quantum cryptography using maximally entangled qubits,” in *IEEE GLOBECOM*, 2020, pp. 1–6.
- [35] M. Sasaki, M. Fujiwara, H. Ishizuka, W. Klaus, K. Wakui, M. Takeoka, S. Miki, T. Yamashita, Z. Wang, A. Tanaka *et al.*, “Field test of quantum key distribution in the Tokyo QKD Network,” *Optics Express*, vol. 19, no. 11, pp. 10 387–10 409, 2011.
- [36] E. Schoute, L. Mancinska, T. Islam, I. Kerenidis, and S. Wehner, “Shortcuts to quantum network routing,” *arXiv preprint arXiv:1610.05238*, 2016.
- [37] S. Shi and C. Qian, “Concurrent entanglement routing for quantum networks: Model and designs,” in *ACM SIGCOMM*, 2020, pp. 62–75.
- [38] P. Shor, “Algorithms for quantum computation: discrete logarithms and factoring,” in *IEEE FOCS*, 1994, pp. 124–134.
- [39] R. Van Meter, “Quantum networking and internetworking,” *IEEE Network*, vol. 26, no. 4, pp. 59–64, 2012.
- [40] R. Van Meter and J. Touch, “Designing quantum repeater networks,” *IEEE Communications Magazine*, vol. 51, no. 8, pp. 64–71, 2013.
- [41] G. Vardoyan, S. Guha, P. Nain, and D. Towsley, “On the stochastic analysis of a quantum entanglement distribution switch,” *IEEE Transactions on Quantum Engineering*, vol. 2, pp. 1–16, 2021.
- [42] M. Victora, S. Krastanov, A. S. de la Cerda, S. Willis, and P. Narang, “Purification and entanglement routing on quantum networks,” *arXiv preprint arXiv:2011.11644*, 2020.
- [43] B. M. Waxman, “Routing of multipoint connections,” *IEEE Journal on Selected Areas in Communications*, vol. 6, no. 9, pp. 1617–1622, 1988.
- [44] Y. Ye and P. M. Pardalos, “A class of linear complementarity problems solvable in polynomial time,” *Linear Algebra and Its Applications*, vol. 152, pp. 3–17, 1991.
- [45] J. Yin, Y. Cao, Y.-H. Li, S.-K. Liao, L. Zhang, J.-G. Ren, W.-Q. Cai, W.-Y. Liu, B. Li, H. Dai *et al.*, “Satellite-based entanglement distribution over 1200 kilometers,” *Science*, vol. 356, no. 6343, pp. 1140–1144, 2017.
- [46] S. B. Yoo and P. Kumar, “Quantum wrapper networking,” in *IPC*. IEEE, 2021, pp. 1–2.
- [47] Y. Zeng, J. Zhang, J. Liu, Z. Liu, and Y. Yang, “Multi-entanglement routing design over quantum networks,” in *IEEE INFOCOM*, 2022.
- [48] Y. Zhao and C. Qiao, “Redundant entanglement provisioning and selection for throughput maximization in quantum networks,” in *IEEE INFOCOM*, 2021, pp. 1–10.
- [49] Y. Zhao, G. Zhao, and C. Qiao, “E2E fidelity aware routing and purification for throughput maximization in quantum networks,” in *IEEE INFOCOM*, 2022.



Huayue Gu (Student Member 2021) received her M.S. degree from the University of California, Riverside, CA, USA, in 2021. Currently, she is a Ph.D. student in the Computer Science department at North Carolina State University. Her research interests are quantum networking, quantum communication, data analytics, etc.



Zhouyu Li (Student Member 2021) received his B.S. degree from Central South University, Changsha, China, in 2019 and his M.S. degree from Georgia Institute of Technology, Atlanta, U.S., in 2020. Currently, he is a Ph.D. student of Computer Science at North Carolina State University. His research interests include privacy, cloud/edge computing, network routing, etc.



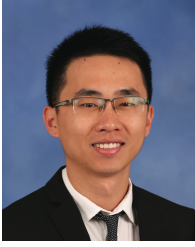
Ruozhou Yu (Student Member 2013, Member 2019, Senior Member 2021) is an Assistant Professor of Computer Science at NC State University, USA. He received his PhD degree (2019) in Computer Science from Arizona State University, USA. His research interests include quantum networking, edge computing, algorithms and optimization, distributed learning, and security and privacy. He has served or is serving on the organizing committees of IEEE INFOCOM 2022–2023 and IEEE IPCCC 2020–2023, as a TPC Track Chair for IEEE ICCCN 2023, and as members of the technical committees of IEEE INFOCOM 2020–2023 and ACM Mobihoc 2023. He received the NSF CAREER Award in 2021.



Xiaojian Wang (Student Member 2021) received her B.E. degree from Taiyuan University of Technology, China, in 2017 and received her M.S. degree in Computer Science from University of West Florida, FL, USA and Taiyuan University of Technology, China, in 2020. She is now a Ph.D. student in the department of Computer Science, College of Engineering at North Carolina State University. Her research interests include payment channel network, security, blockchain, and so on.



Fangtongzhou (Student Member 2021) received her B.E. degree (2018) in Electrical Engineering and Automation from Harbin Institute of Technology, Harbin, China and M.S. degree (2020) in Electrical Engineering from Texas A&M University, College Station, Texas, USA. Currently she is a Ph.D candidate in the School of Computer Science at North Carolina State University. Her research interests include machine learning in computer networking, like federated learning, reinforcement learning for resource provisioning, etc.



Jianqing Liu (Member 2018) is currently an Assistant Professor at the Department of Computer Science at NC State University. He received the Ph.D. degree from The University of Florida in 2018 and the B.S. degree from University of Electronic Science and Technology of China in 2013. His research interest is wireless communications and networking, security and privacy. He received the U.S. National Science Foundation Career Award in 2021. He is also the recipient of several best paper awards including the 2018 Best Journal Paper Award from IEEE Technical Committee on Green Communications & Computing (TCGCC).